I J C T A, 9(5), 2016, pp. 2705-2715

Switched Reluctance Machine using Modified Magnetic Circuit with Generation Capabilities

Rajmal Joshi M.* and Dhanasekaran R.**

ABSTRACT

The concept of dual air-gap to improve the torque density of the switched reluctance machine is attempted by researchers recently. The dual air-gap machine is able to produce higher average torque compare to the conventional machine; however its weakness is the increase in the volume of the machine that leads to a heavier motor application. Therefore, a novel design through modification on magnetic circuit of the dual air-gap in double rotor switched reluctance machine is proposed. In this paper the detailed analysis of the proposed structure and its operating characteristics are investigated and reported. The torque density of the proposed machine is 35% higher than the conventional machine while the motor constant square density increased by 64%. The volume of the proposed machine is reduced by 6.6% with SRM.

Keywords: grand challenges, sustainable strategy, engineering solutions, grand challenges.

1. INTRODUCTION

A traction motor is usually controlled through the terminal voltage as speed is varied from minimal to its nominal speed in a constant uniform magnetic field [1]. After the nominal speed with constant terminal voltage, the magnetic field is weakened towards the critical speed before breaking down. Figure.1 shows the typical torque power speed characteristics required for traction motor. For EV applications the constant power range need to be extended for better efficiency and control [2]. Table 1 shows the electric vehicle models developed by various manufacturers.

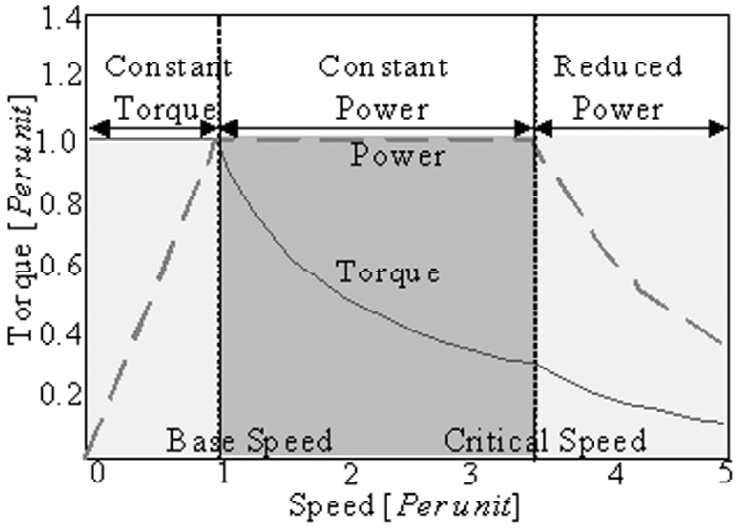

Figure 1: Torque Power Characteristics of the EV [2]

* Research Scholar, Sathyabama University, Chennai, India, *Email: rajmaljoshi@gmail.com*

** Director Research, Syed Ammal Engineering College, Ramanathapuram, India, *Email: rdhanashekar@yahoo.com*

Table 1
Electric vehicle models

Type of Motor	*Manufacturer*	*Name*
DC Motor	Fiat	Elettra
	Mazda	Bongo
	Conceptor	G-Van
PMDC motor	Suzuki	Senior tricycle
Induction motor	Fiat	SeicentoElettra
	Ford	Think city
	General Motors	EV1
PMSM	Hondo	EV Plus
	Nissan	Altra
	Toyota	RAV4
SRM	Lucas	Chloride
PM BLDC	Toyota	Prius
	Honda	Civic

Conventionally the magnet controlled machines are used due to its higher power density. DC motor drives are the primary choice for such applications as high torque at low speed is best possible, however it drags rapid maintenance. Brushless DC machines (BLDC) in most modern on-road vehicles due to their maintenance free operation. Equally modern vehicles encompass Permanent Magnet Synchronous Machines (PMSM) as alternative due to their higher efficiency and power density over other type of electric motors [2-3]. The prime challenge of this machine is the flux weakening control at constant power high speed region. Induction motors is disadvantageous due to low efficiency due to the motor losses due the winding losses in the stator and rotor together with the challenge in recovering energy during braking.

Moving forward the usage on the high volume of the rare earth permanent magnet motors would push the motor manufacturers to the choice of the magnet less machines in the near future. Switched Reluctance Machine (SRM) though simple in construction their design and control are challenging making it not the prime choice for commercial deployment [4-6]. Hence the key design challenges in the magnet-fewer machines is the optimal utilization of steel and copper, better electromagnetic flux flow, the machine topology and geometry to increase the torque per unit weight. Recently the dual magnetic circuit design through double stator is proposed in [7-8] and through the double rotor is introduced in [9].

Dual magnetic circuit can be done through introducing either a double stator configuration or through double rotor configurations [8] and phase displacement in [9]. In the double stator structure the electrical loading is doubled however it do not improve the efficiency as the resistance value increases and hence the copper loss. Also it increases the mass of the vehicle when the machine is on board, regenerative action invokes the reverse effect on the current flow in the two winding coil increasing the mutual inductance effect on the machine. This paper presents the dual circuit realization through a modified switched reluctance machine with capability for generation capability. The design aspects, the magnetic circuit analysis using FEA tool and its performance analysis is presented.

2. METHODOLOGY

2.1. Design Aspects

2.1.1. Design Approach

Figure 2 shows the methodology used in this research design. The conventional SRM [10] is designed and tested for the performance analysis of torque and power output based on the design procedure presented in

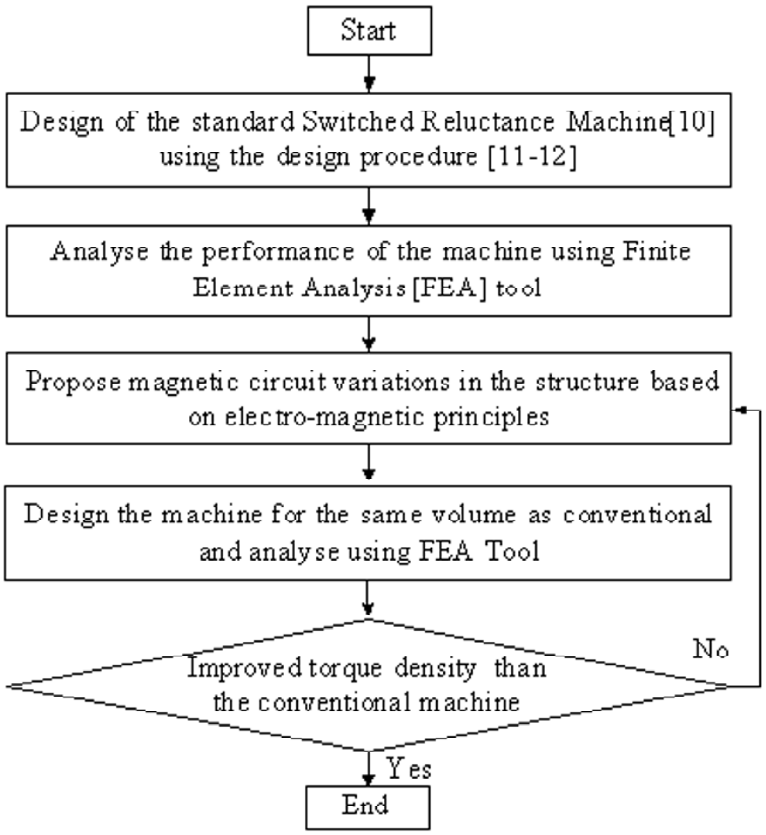

Figure 2: Methodology used in this research design

[11-13]. Then, the geometrical design based on the electro-magnetic principles is proposed, mathematically analyzed and is simulated to test the performance of the machine. Both the machines are designed for the same volume in order for the comparison to be genuine.

Figure 3(a) shows the conventional reluctance machine magnetic circuit and figure 3(b) shows the magnetic circuit expansion of the conventional machine, which can be realized as two stators or as two rotors. However using a dual stator increase the windings, the resistance increases and thereby decreases the efficiency of the machine. Hence a double rotor is viable solutions whereby the application that require

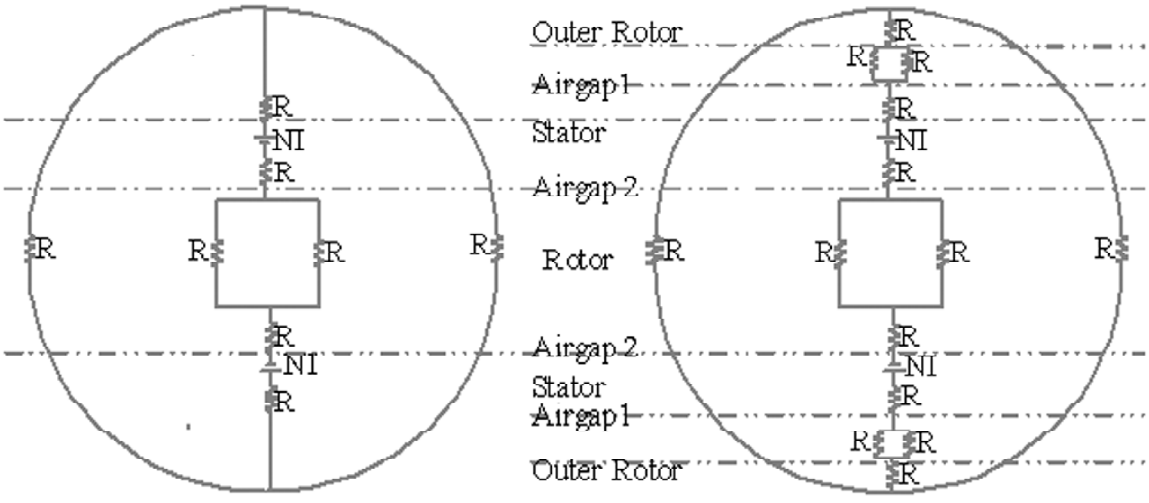

(a) Conventional SRM **(b) Proposed SRM**

Figure 3: Conventional and proposed SRM

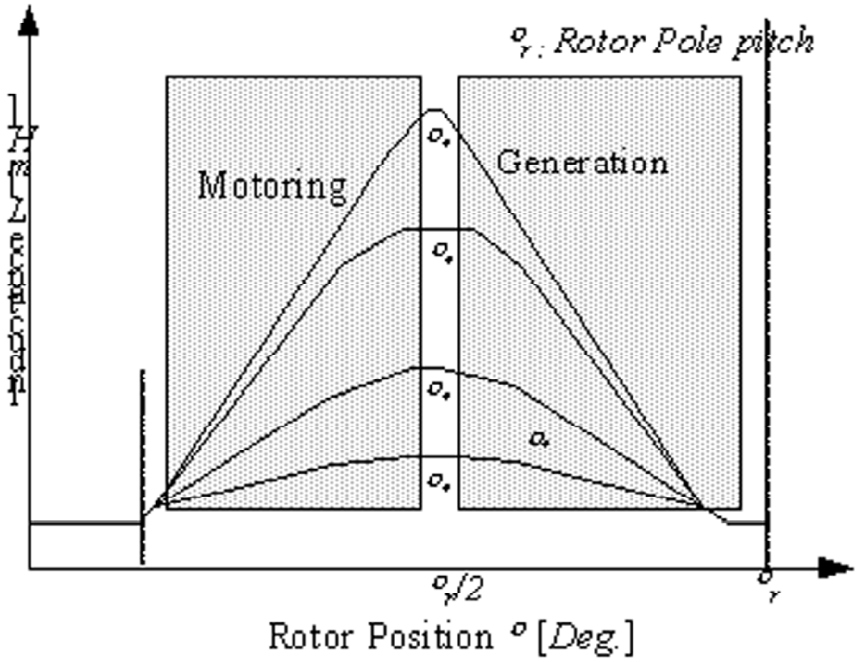

Figure 4: SRM operating capability

motor generator operation when operating as independent. This is similar to that of the flywheel concept used in the vehicle applications. This motivated the use of dual rotor that is designed which can be either used in tandem or independently, which could be done using a controller. As seen in the figure 3 there are two airgap and thereby the flux control is possible with the way the machine is operated. In case of application such as wind turbine where the speed of wind velocity is low speed to high speed thereby the use of rotor with different diameter the power generated is controlled. Figure 4 shows the typical inductance characteristics various current excitations for rotor position under motoring and braking (generation) and is influenced by the position of the rotor with respect to the rotor.

2.1.2. Sizing of the Machine

The relation of output is calculated from its machine size, machine volume, machine speed, specific magnetic loading and specific electric loading [12]. The output equation, Q is given in Equation (1)

$$Q = n_{ph} E_{ph} I_{ph} \times 10^{-3} \tag{1}$$

where E_{ph} is the voltage output per phase and I_{ph} is the current per phase. Since there is only a single electric circuit for each phase, the current per phase, I_{ph} and current carrying conductor, I_z have an equal value. Ihe output voltage per phase, E_{ph} to the induced emf per phase is shown in Equation (2)

$$E_{ph} = 4.44 \frac{p_s n}{2} \phi T_{ph} K_w \tag{2}$$

where n is the rotating speed in revolution per second (*rps*), p_s is the number of poles, ϕ is the magnetic flux in the coil. Since the output voltage per phase, E_{ph} is related to the output equation, the output equation is given again in Equation (3).

$$Q = 1.11\, K_w \times (2 n_{ph}\ T_{ph})\ (p_s \phi) \times (p_s \phi) \times I_z \times 10^{-3} \tag{3}$$

where K_w is the winding factor. The output equation is further simplified and it is given in Equation (4)

$$Q = n C_o D_{or}^{\ 2} L_{st} \tag{4}$$

where D_{or} is the rotor diameter, L_{st} is the stack length and C_o is the output coefficient, given in Equation (5)

$$C_o = 11\, B_{av} ac K_w \times 10^{-3} \tag{5}$$

where B_{av} is specific magnetic flux density, ac is specific electric loading. Table II shows the designed machine values and Figure 5 shows the proposed machine in exploded view.

2.1.3. Magnetic Flux Analysis

Figure 6 shows the magnetic flux flow at various position of the machine. The analysis is done for one rotor pole pitch and it is found the flux flow is uniform and the leakage is minimal. For electric vehicle operation it is highly important the recovery of energy during the braking (regeneration). Hence improving torque density with low ripple to a lower value make SR machines a significant choice for battery operated electric vehicles [14].

Table 1
Designed Machine values

Parameter	*Value*
Diameter of outer rotor	80.0 mm
Stack length	50.0 mm
Diameter of outer rotor bottom suface	65.7 mm
Diameter of outer stator	65.6 mm
Diameter of inner stator	25.0 mm
Diameter of inner rotor	24.9 mm
Diameter of circular hole	2.0 mm
Diameter of shaft	14.0 mm
Pole arc of outer rotor	35 deg
Pole arc of inner rotor	42 deg
Pole arc of inner stator	40 deg
Pole arc of outer stator	50 deg
Inner air-gap length	0.1 mm
Outer air-gap length	0.1 mm

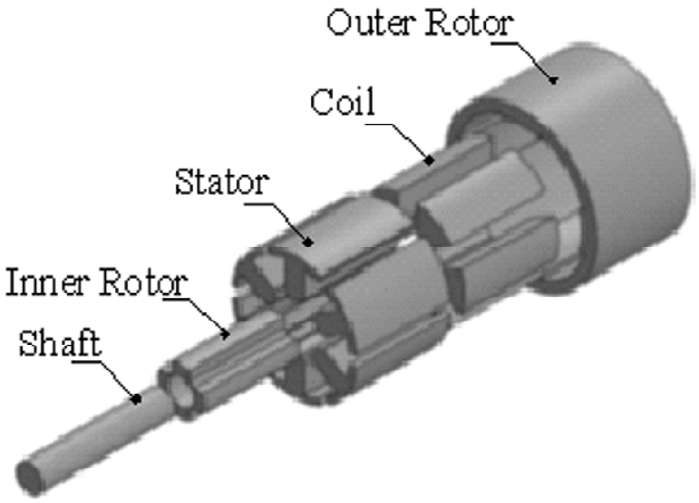

Figure 5: Proposed machine in exploded view

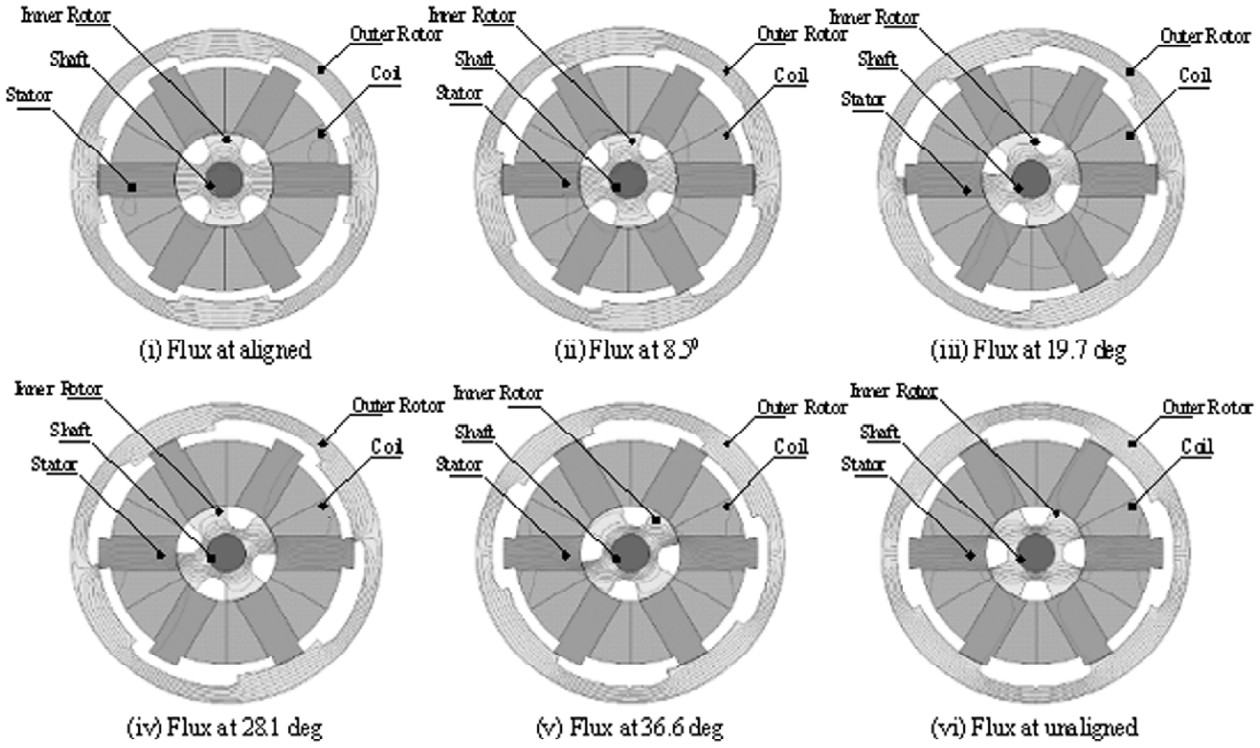

Figure 6: Magnetic flux at various positions used to compute inductance characteristics

2.1.4. Evaluation Parameter

For a comparatively study the performance the following parameters are used [13].

A. Motor Constant Square Density (G)

The motor constant square density is one of the quality factors for comparison of machines as it involves the comparison based on the sizing of the machines is as in Equation (6)

$$G = \frac{K_m^2}{V} \tag{6}$$

where K_m is the machine constant $\left(= \frac{K_t}{\sqrt{P_{in}}} \right)$; K_t is the torque constant $\left(= \frac{T_{ave}}{I} \right)$ in [$Nm/A/W^{-(1/2)}$], V is the volume of the machine [m^3], T_{ave} is the average torque, P_{in} being the input electrical power.

B. Torque per Unit Volume (T_{mv})

The torque per unit volume for variable size in terms of volume is shown in Equation (7)

$$T_{mv} = \frac{4\ T_{ave}}{\pi\ D_{or}^2 L_{sk}} \tag{7}$$

where D_{or} is the diameter of the outer rotor, L_{sk} is the stack length

C. Ripple Factor (γ_{rf})

The peak variations of the torque over a full cycle of operation of a motor is expressed as ripple factor as shown in Equation (8).

$$\gamma_{rf} = \frac{T_{\max} - T_{\min}}{T_{ave}} \tag{8}$$

where T_{max} is the torque maximum of the machine, T_{min} is the torque minimum of the machine,

D. Total Harmonic Distortion (THD)

THD is used to assess the signal distortion by cause of oscillations at output harmonics characteristics is as shown in Equation (9).

$$THD = \frac{\sqrt{\sum_{i=2}^{\infty} T_i^2}}{T_1} \tag{9}$$

where T_1 is the fundamental torque of the machine.

3. RESULTS AND DISCUSSIONS

3.1. Static Characteristics

The flux linkage waveform of the proposed machine when excited with current of 3A, 5A, 7A is as shown in Figure 7(a). Close to the half pole pitch the magnetic flux is constant and hence need to use controller to switch on the next phase. This information is highly helpful in the design of the controller at later stage. Figure 7(b) shows the inductance characteristics for the proposed machines. In traction applications the large dead zone enables larger phase advance control so that the current the torque is proportioned when the rotor speed is above the nominal speed. This is realized with smaller pole arc at unaligned position and small air gap at aligned position that is seen in out design here.

3.2. Dynamic Characteristics

The excitation state is based on the position of switches relative to that of the position of the rotor. During the excitation state of the switches, a significant increase in the average torque value and hence

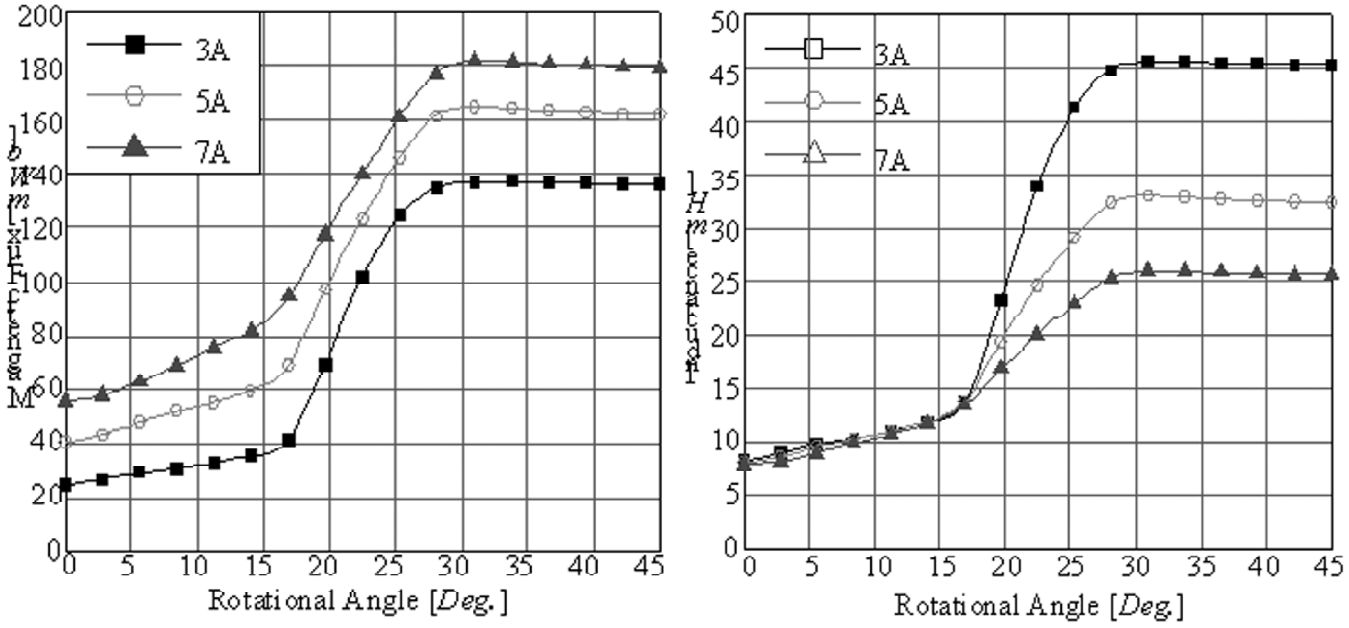

(a) Magnetic flux characteristics **(b) Inductance characteristics**

Figure 7: Electro-magnetic characteristics of the machine

the torque constant. Figure 8(a) shows the drive and the switching pattern used for the drive is shown in Figure 8(b).

Figure 9(a) shows the speed torque characteristics of the proposed machines as the speed is varied from 0 to 2400 rpm.For the four rotors pole with dual the speed settles close to 1500 rpm reaching torque close to 2.1 Nm. The maximum torque achieved is about 2.4 Nm. Figure 9(b) shows the efficiency is rises and reach maximum of 90. The increase in the efficiency is the frequency of the switched that is set with the accordance of rotation speed. An advanced phase angle switching is equally relevant in this case to reduce ripple [14].

Figure 10(a) shows the timing control used in the generating conditions. Figure 10(b) shows the toque characteristics used for analysis of the machine for consideration during regeneration. It is found the ripple is reduced when the angle of control is between 55^0-57^0 during regeneration and 10^0-12^0 during motoring.

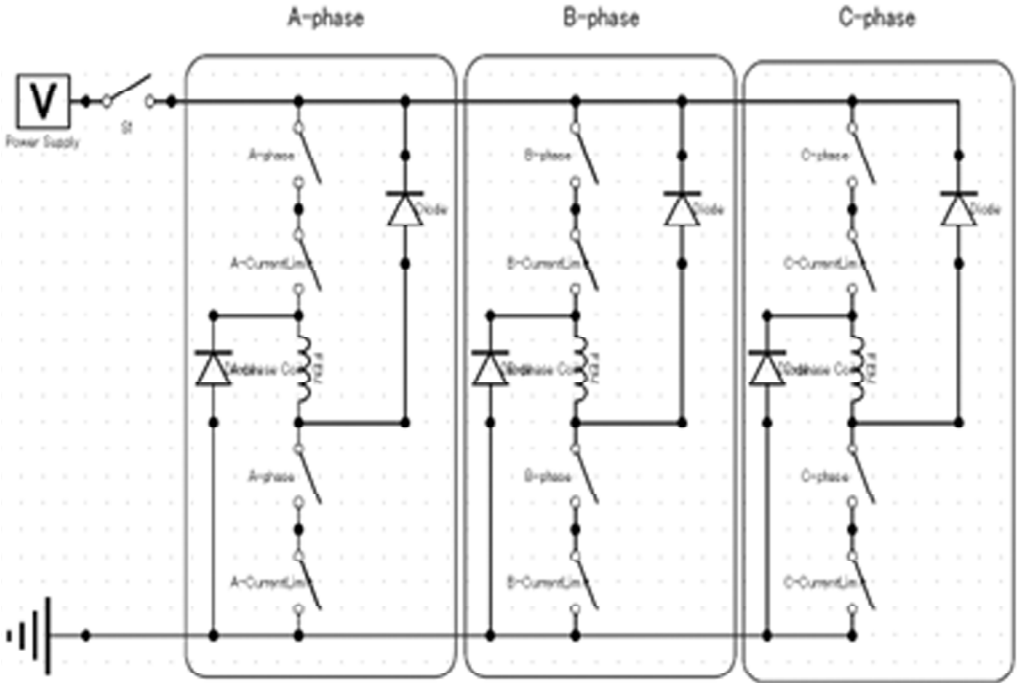

(a) Drive circuit diagram.

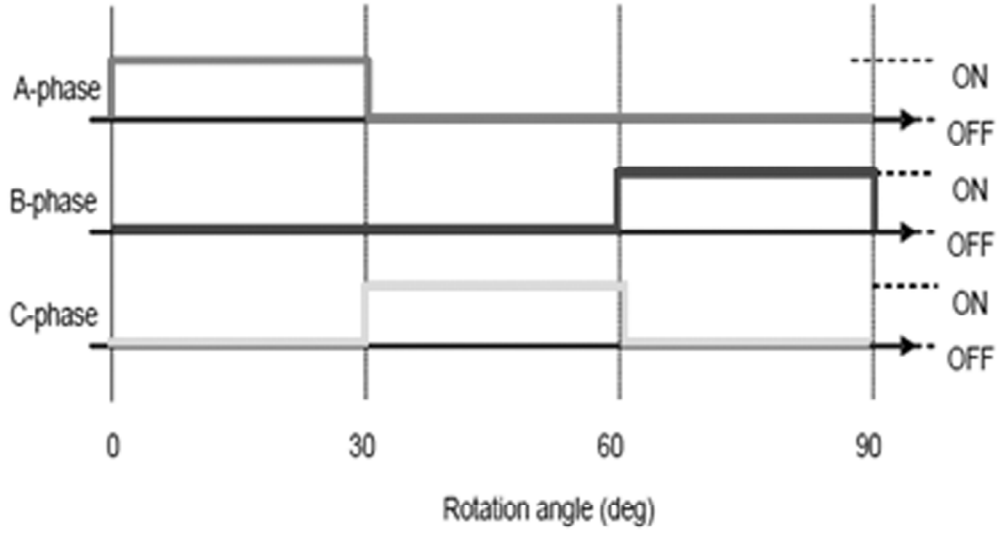

(b) Drive switched timing chart.

Figure 8: Drive switching used.

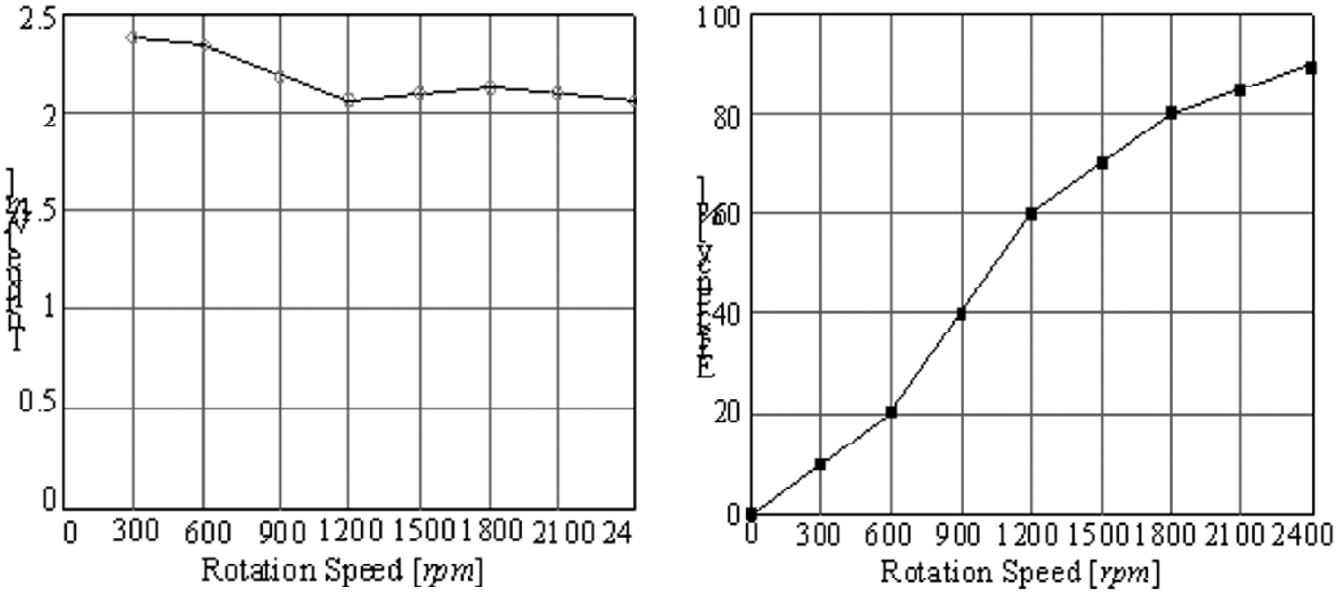

(a) Speed torque characteristics **(b) Efficiency versus speed**

Figure 9: Output characteristics of the machine

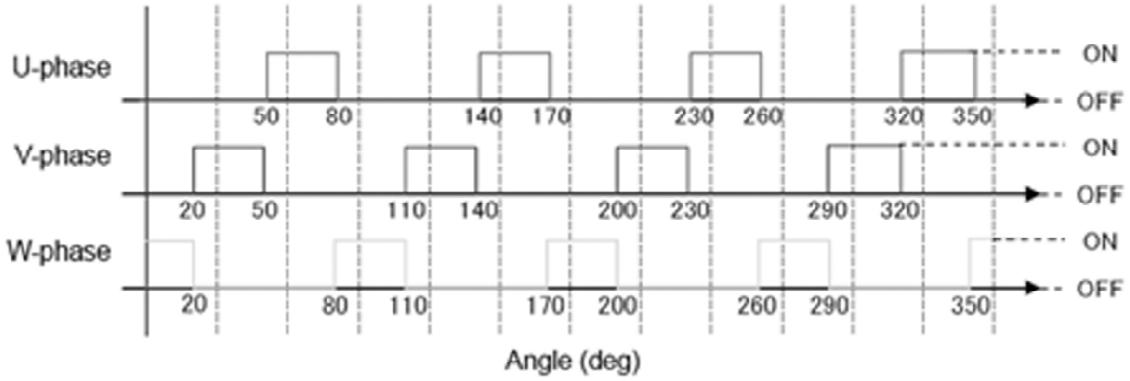

(a) Ripple torque switch timing table

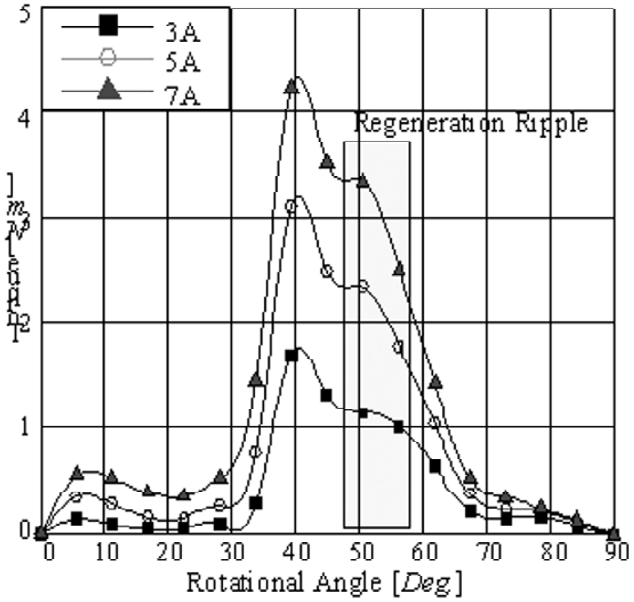

(b) Ripple during regeneration

Figure 10: Generation capability of the proposed machines

E. Comparative Evaluations

Table III shows the comparative evaluations of the conventional and the proposed machine. Both machines are designed for same sizing and procedure. As seen from the results the comparison is made for the same volume, since no magnetic field from magnet is involved the electrical loading is decreased in DRSRM due to the space required for the second rotor. However the air gap is doubled, the net air gap length in both the machines are the same. The torque density is increased by 66% and the motor constant square density is increased by 64%. As mentioned earlier the motor constant square density is the best figure of merit to compare as it involves the volume and weight of the machines. The average torque in case of the DRSRM is increase by 35% as subsequently the analysis of the ripple is presented.

Table 2
Comparative evaluations

Figure of Merit	Conventional	Proposed
Current, i[A]	5	5
Volume, V[m^3]	$2.13e^{-3}$	$1.99e^{-3}$
T_{avg}[Nm]	1.26	1.98
T_{max}[Nm]	1.656	2.418
T_{min}[Nm]	1.652	2.170
γ_{rf}	$3.2e^{-3}$	0.13
T_{mv}[Nm/m^3]	2366.2	**3979**
K_t[Nm/A]	0.13	0.20
K_m[$Nm/A/W^{-\left(\frac{1}{2}\right)}$]	0.013	0.020
G[$(Nm)^2/A^2/W/m^3$]	0.07	**0.20**

4. CONCLUSION

Switched reluctance machines are viable candidate as with proper control and extended power range without multi-gear transmission. A dual magnetic circuit is realized through double rotor structure and the static and dynamic performance is presented. The proposed machine is compared with that of the conventional machines through motor constant square density, a factor used to compare for the same volume. The torque density of the proposed machine is 35% higher than the conventional machine while the motor constant square density increased by 64%. The ripple is reduced at the operation of the angle is done at 55^0-57^0 during regeneration and 10^0-12^0 during motoring. The proposed machine is showing as a viable alternative for the EV and HEV applications to that of brushless and permanent magnet machines..

REFRENCES

1] Ehsani, M.; Yimin Gao; Gay, S., "Characterization of electric motor drives for traction applications," *Industrial Electronics Society, The 29th Annual Conference of the IEEE*, vol.1, pp. 891, 896, 2-6 Nov. 2003

[2] Chu, C.L.; Tsai, M.C.; Chen, H.Y., "Torque control of brushless DC motors applied to electric vehicles," *Electric Machines and Drives Conference, IEEE International*, pp. 82,87, 2001.

[3] Wang, T.; Cheng, M.; Fan, Y.; Chau, K.T, "A double stator permanent magnet brushless machine system for electric variable transmission in hybrid electric vehicles," in Proc. 2010 IEEE Vehicle Power Propulsion Conf., pp. 1-5, Sep 1-3 2010.

[4] Hu, K.; Yi, P.; Liaw, C., "An EV SRM Drive Powered by Battery/Supercapacitor withG2V and V2H/V2G Capabilities," *Industrial Electronics, IEEE Transactions on*, vol. 99, pp. 1-11, 2015

[5] Aida, S.; Komatsuzaki, A.; Miki, I., "Basic characteristics of electric vehicle using 40kW switched reluctance motor," *Electrical Machines and Systems, International Conference on*, pp. 3358, 3361, 17-20 Oct. 2008.

[6] Jazdzynski, W.; Majchrowicz, M., "An approach to find an optimum designed SRM for electric vehicle drive," *Electrical Machines, 18th International Conference on*, pp. 1, 6, 6-9 Sept. 2008.

[7] Abbasian, M.; Moallem, M.; Fahimi, B., "Double-Stator Switched Reluctance Machines (DSSRM): Fundamentals and Magnetic Force Analysis," *Energy Conversion, IEEE Transactions on*, vol. 25, no.3, pp. 589, 597, Sept. 2010.

[8] Wei Peng.; Dong-Hee, Lee.; Fengge, Zhang.; Jin-Woo, Ahn., "Design and characteristic analysis of a novel bearingless SRM with double stator," *Electrical Machines and Systems (ICEMS), 2011 International Conference on*, pp. 1, 6, 20-23 Aug. 2011.

[9] Aravind, CV.; Norhisam, M.; Aris, I.; M.H., Marhabhan., "Double Rotor Switched Reluctance Motors: Fundamentals and Magnetic Circuit Analysis" IEEE Student Conference on Research and Development, Malaysia, pp. 294-299, 19-20 Dec. 2011.

[10] K. T. Chau, "Switched Reluctance Motor Drives," in *Electric Vehicle Machines and Drives: Design, Analysis and Application* , 1, Wiley-IEEE Press, 2015, pp. 375-doi: 10.1002/9781118752555.ch5

[11] Aravind, C.V.; Norhisam, M.; Firdaus, R.N.; Aris, I.; Marhaban, M.H.; Nirei, M., "Analysis on the torque characteristics due to outer rotor displacement in the double rotor switched reluctance machine," Power Electronics and Drive Systems (PEDS), IEEE 10th International Conference on, pp. 773,777, 22-25 April 2013.

[12] Aravind Vaithilingam "Design of Electrical Apparatus" *Charulatha Publications*, Chennai, 2003.

[13] Aravind, C.; Norhisam, M.; Aris, I.; Marhaban, M.H.; Nirei, M., "Static characteristics of the double rotor switched reluctance motor," *Power and Energy (PECon), IEEE International Conference on*, pp. 402,407, 2-5 Dec. 2012.

[14] Hongwei, Gao.; Yimin, Gao.; Ehsani, M., "A neural network based SRM drive control strategy for regenerative braking in EV and HEV," *Electric Machines and Drives Conference. IEEE International*, pp. 571, 575, 2001.